Available online at www.sciencedirect.com

ScienceDirect

Procedia Structural Integrity 33 (2021) 347–356

Structural Integrity Procedia

www.elsevier.com/locate/procedia

IGF26 - 26th International Conference on Fracture and Structural Integrity

An innovative nondestructive technique for the local assessment of residual elastic properties in laminated composites

C. Boursier Niutta[a*], A. Tridello[a], G. Belingardi[a], D.S. Paolino[a]

[a]*Politecnico di Torino, Corso Duca degli Abruzzi, 24, Turin, 10129, Italy*

Abstract

In this work, an innovative experimental methodology is presented for the assessment of damage severity in composites. The technique aims at determining the local variation of the elastic properties in the damaged region of a composite component. Based on the Impulse Excitation Technique (IET), the vibrational response of the inspected region is isolated by clamping its extremities through vacuum, thus allowing the assessment of local variations. Complementarily, a new analytical approach is derived for the assessment of the residual elastic properties of the damaged area from the measurement of the first resonant frequency. Validation of the proposed methodology is performed on two glass-fibre woven fabric composites, damaged by impact. The material properties of the damaged zone determined through the proposed technique are compared to the results of tensile tests performed on specimens cut from the impacted plates. In particular, the specimens are equipped with optic fibre in order to punctually measure the elastic parameters. Results show that the residual elastic properties assessed with the proposed technique are in very good agreement with those measured through the optic fibre, thus proving the effectiveness of the methodology.

Keywords: Laminated Composites; Damage Severity Assessment; Impulse Excitation Technique; Local Elastic Properties

* Corresponding author.
E-mail address: carlo.boursier@polito.it

10.1016/j.prostr.2021.10.042

1. Introduction

In order to design safer and more cost-effective composite structures, damage tolerance strategies, based on a proper combination of material behaviour description and nondestructive techniques, are required. Anomalies in the structural integrity of composites can arise both during the manufacturing process and during the service life. These anomalies can concern specifically the matrix, i.e., voids, uncured region or matrix cracking, the fibre, i.e., fibre misalignment, fibre waviness or broken fibres, and the matrix/fibre interface, i.e., matrix/fibre debonding or laminae debonding. This rich collection of failure mechanisms usually combines in a complex multitude of cracks and flaws, which demand for a proper assessment of their severity. Historically, damage severity is determined in terms of extension of the cracked area. Indeed, in metals, a residual strength can be correlated to the most "critical" crack, thus estimating the damage severity. However, due to their heterogenous nature and to their anisotropy, strength degradation approaches are not suitable for composites. Given the complex crack scenario typical of composites, it is not a priori known which is the direction of minimum strength [1].

These observations suggest the need to assess the damage severity in terms of material response in presence of defects or flaws, rather than only in terms of extension of the damaged area. Generally speaking, the presence of cracks, voids, impact damages etc., results in a local variation of the elastic properties, whose assessment constitutes a suitable metric for damage severity. However, current nondestructive techniques either lack a quantitative assessment of the elastic constants, as in the case of thermography or micro-CT methods [2], or are likely to conceal the damage identification, as in the case of vibrational methods where the global vibrational response is analyzed [3–5].

In this work, an innovative nondestructive technique is presented for the assessment of residual elastic properties in damaged laminates. The technique is based on the Impulse Excitation Technique (IET) [6] and differently from global vibrational methods [7], investigates the local vibrational response of the component, thus assessing the local material response [8,9]. In particular, the inspected region is isolated by nondestructively clamping its boundaries, and, with reference to the first resonant frequency, a vibrational mode is excited, which is function of only the material characteristics of the investigate region. Complementarily, a new analytical approach is derived for the assessment of the residual elastic properties of the damaged area from the measurement of the first resonant frequency. Validation of the proposed methodology is performed on two glass-fibre woven fabric composites damaged by impact. The material properties of the damaged zone determined through the proposed technique are compared to the results of tensile tests performed on specimens cut from the impacted plates. In particular, the specimens are equipped with an optic fibre in order to punctually measure the longitudinal strain and so the elastic parameters.

Nomenclature

E_{11}	longitudinal Young's modulus
E_{22}	transverse Young's modulus
G_{12}	in-plane shear modulus
ν_{12}	in-plane Poisson's coefficient
f_0	first resonant frequency of the undamaged material
f_d	first resonant frequency of the damaged material

2. Materials and Methods

2.1. Materials

Experimental tests are performed on two laminated composite plates manufactured in the laboratory of Politecnico di Torino. The two laminates are made of glass fibre woven fabric impregnated with epoxy resin. The first composite laminate consists of 6 layers, whereas the second is made of 8 layers. The glass fabric is a twill 2x2 with slightly different fibre concentrations in the two perpendicular directions. In particular, the yarn densities are

11.5 and 12 fibre/mm in the warp and weft directions, respectively. The laminates are produced by vacuum infusion, with the glass fabric plies stacked in parallel. The curing process is accomplished in oven at 100°C for 3 hours without providing any adding pressure. The stacking sequence is $[0]_6$ for the 6-layers plate and $[0]_8$ for the 8-layers plate. In regard to the thickness, the 6-layers plate is 1.31 mm thick, whereas the 8-layers plate 1.24 mm. A larger amount of resin is thus present in the 6-layers plate. The resulting elastic properties, assessed through tensile tests, are reported in Table 1 for the two plates with reference to the material orthotropy axes.

Table 1. Material properties of the 6- and 8-layers plates.

	Property	Value	Unit
6-layers plate	Density	$1.5 \cdot 10^3$	kg/m^3
	E_{11}	17.5	GPa
	E_{22}	16.7	GPa
	G_{12}	3.1	GPa
	ν_{12}	0.13	-
8-layers plate	Density	$1.66 \cdot 10^3$	kg/m^3
	E_{11}	21.5	GPa
	E_{22}	19.5	GPa
	G_{12}	3.7	GPa
	ν_{12}	0.17	-

2.2. Methods

In this Section, the methodology is described. Firstly, the experimental setup which clamps the boundaries from only one side is presented. Then, the numerical calculations for the assessment of the residual elastic properties of the damaged zone are detailed.

Experimental setup of the nondestructive technique

In order to restrict the mechanical vibrations to a subregion of the component, i.e., only the subregion is involved in the vibrational phenomenon, its boundaries must be clamped. As shown in Fig. 1 through a finite element model, differently from simply supported boundaries, the clamped constraint allows to isolate a vibrational mode specific of the inspected region and which is function of only its material characteristics.

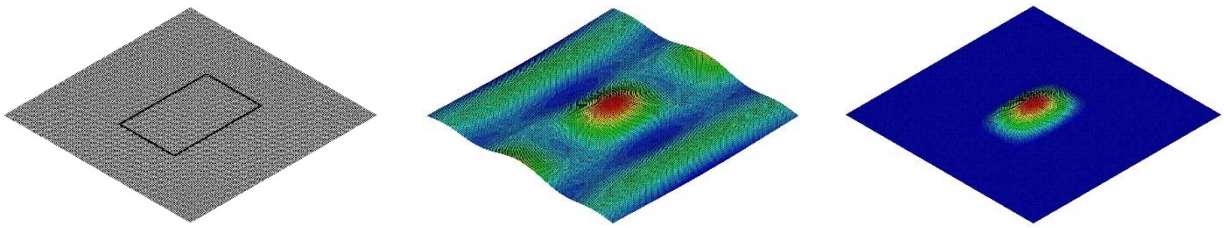

Fig. 1. Comparison of simply supported and clamped boundaries: (a) finite element model with the highlighted boundary nodes, (b) modal analysis with simply supported boundaries (c) modal analysis with clamped boundaries.

In order to nondestructively clamp the boundaries, vacuum is adopted. Fig. 2a shows the experimental setup, while the device is presented in Fig. 2b.

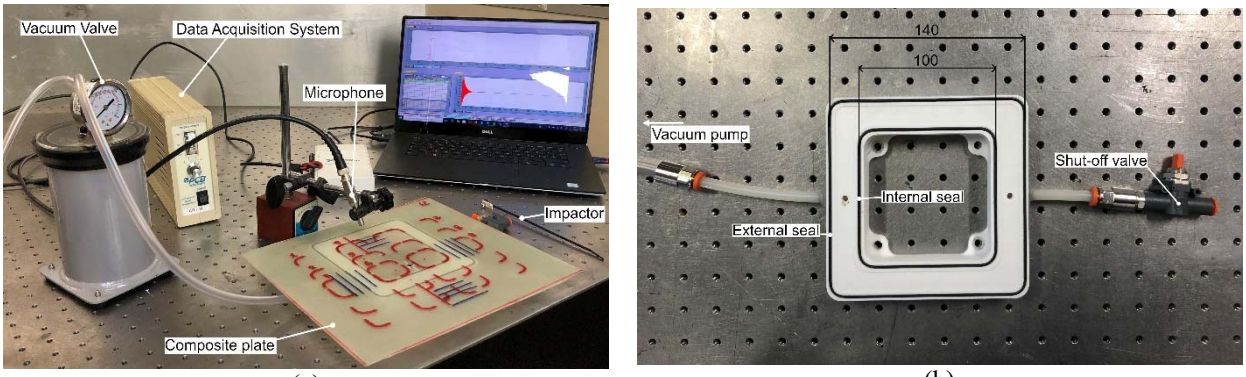

(a) (b)

Fig. 2. (a) Experimental setup; (b) Clamping system: dimensions and details of the vacuum system.

The device is 3D printed and is made of polyethylene terephthalate (PET). As shown in Fig. 2b, the device has a frame shape, and the vacuum is realized in the thin chamber comprised between the external and internal seals by means of a vacuum pump. A shut-off valve is also adopted in order to facilitate the entrance of the air once the measurement is performed. The region under investigation is thus limited by the internal seal, which has square shape of dimension $a = 100$ mm.

It is worth noticing that the presence of the seals affects the stiffness of the boundaries and in turn the resultant resonant frequency, which will be smaller than the resonance of the fully clamped. However, for the local investigations, it is required that the vibrational response must be mostly related to the inspected region, with limited influence of the excluded surrounding material.

The methodology is based on the IET. An impulser is used to excite the plate and the resulting mechanical vibrations are measured through a microphone. The acquisition system (National Instruments NI USB-6210) receives the signal, and the analyser (Buzz-o-sonic®) provides the fundamental resonant frequency through a Fast Fourier Transform of the signal. The data acquisition system has a sample rate of 25 kHz and the signal is analogic-to-digital converted with a resolution of 16 bits. The analyser performs the Fast Fourier Transform of the signal with a resolution smaller than 1 Hz.

As shown in Fig. 1b, the device is fixed to a working table, in order to avoid vibrations of the whole system, i.e., device and composite plate. Therefore, both sides of the plate are utilized in this preliminary test setup. However, it is worthwhile noticing that the experimental setup can be easily converted in order to limit the nondestructive investigations to only one side of the plate. Indeed, in practical applications, the in-field inspection is usually restricted to the exposed surface.

Damage Characterization

The composite plates are damaged by impact. The incident energy of 1.8 J, i.e., the minimum energy of the drop-dart machine, is considered for both the plates. As the laminates are made of glass fibre, the damage is analysed by simple visual inspection. For both the materials, two main perpendicular cracks developed from the impact, which are shown in Fig. 3 with the related dimensions in millimetres.

The presence of a damage within the region inspected through our device results in a reduction of the first resonant frequency. From the measurement of the first resonant frequency, the residual elastic properties of the retained square region can be determined following Hearmon [10], who extended the formula of the first resonant frequency for isotropic materials proposed by Warburton [11] to orthotropic materials:

$$f = \frac{\lambda}{2\pi} \cdot \sqrt{\frac{1}{\rho \cdot h}} \cdot \sqrt{\frac{D_{11}}{a^4} + \frac{D_{22}}{b^4} + \frac{0.605 \cdot H}{a^2 b^2}} \tag{1}$$

where a and b are the dimensions of the plate, h the thickness, ρ the material density and λ a numerical parameter which depends on the boundary conditions. For instance, for simply supported boundaries, λ is equal to 1, whereas for fully clamped boundaries, its value is 22.37. D_{11}, D_{22} and H are the flexural stiffness terms, defined as:

$$D_{11} = \frac{E_{11} \cdot h^3}{12(1 - \nu_{12} \cdot \nu_{21})}$$
$$D_{22} = \frac{E_{22} \cdot h^3}{12(1 - \nu_{12} \cdot \nu_{21})}$$
$$H = \nu_{12} \cdot D_{22} + \frac{G_{12} \cdot h^3}{6} \tag{2}$$

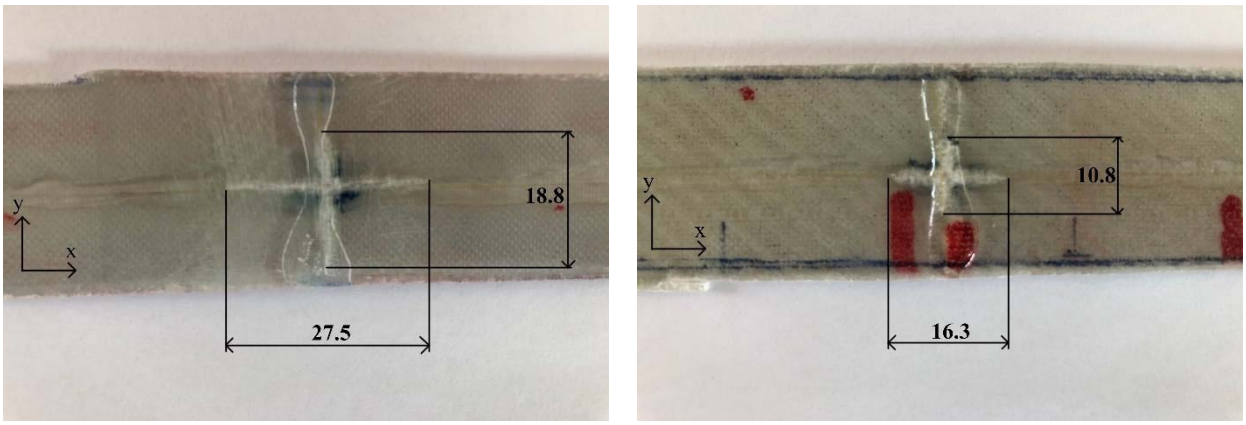

(a) (b)

Fig. 3. Dimensions in mm of the main cracks in (a) 6-layers plate and (b) 8-layers plate.

In an intact plate, the frequency is proportional to the undamaged material properties, i.e., $f_0 \sim \sqrt{D_{11,0} + D_{22,0} + H_0}$, while in presence of a damage, the first resonant frequency is proportional to the residual elastic properties, i.e., $f_d \sim \sqrt{D_{11,eq} + D_{22,eq} + H_{eq}}$. The "$eq$" subscript refers to the so-called equivalent elastic properties. When the damage is comprised within the investigated region, the measurement of the first resonant frequency f_d is the result of the contribution of both the damaged zone, i.e., the area where cracks are confined, and the surrounding intact material.

Therefore, from two measurements of the first resonant frequency, in the undamaged and damaged state, the following relationship between the residual elastic properties of the whole inspected region and the intact ones can be written:

$$\frac{D_{11,eq}}{a^4} + \frac{D_{22,eq}}{b^4} + \frac{0.605 \cdot H_{eq}}{a^2 b^2} = \left(\frac{D_{11,0}}{a^4} + \frac{D_{22,0}}{b^4} + \frac{0.605 \cdot H_0}{a^2 b^2}\right)\left(\frac{f_d}{f_0}\right)^2 \tag{3}$$

and among the infinite possible solutions, we can reasonably assume that:

$$D_{11,eq} = D_{11,0}\left(\frac{f_d}{f_0}\right)^2$$
$$D_{22,eq} = D_{22,0}\left(\frac{f_d}{f_0}\right)^2$$
$$H_{eq} = H_0\left(\frac{f_d}{f_0}\right)^2 \tag{4}$$

Finally, combining Eqs. (2) and (4) and neglecting the variation of the Poisson's coefficient, the residual elastic properties of the whole inspected region can be expressed as:

$$E_{11,eq} = E_{11,0}\left(\frac{f_d}{f_0}\right)^2$$
$$E_{22,eq} = E_{22,0}\left(\frac{f_d}{f_0}\right)^2$$
$$G_{12,eq} = G_{12,0}\left(\frac{f_d}{f_0}\right)^2 \quad (5)$$
$$\nu_{12,eq} = \nu_{12,0}$$

Thereafter, the objective is to determine the residual elastic properties specifically of the damaged region. In this regard, the first resonant frequency is mapped on the plate, for different positions of the damage with respect to the boundaries of the device. In particular, the frequency is mapped in the x direction, as shown in Fig. 4, which refers to one of the orthotropy material direction, here defined as direction 1. The residual properties along this direction are then verified with tensile tests.

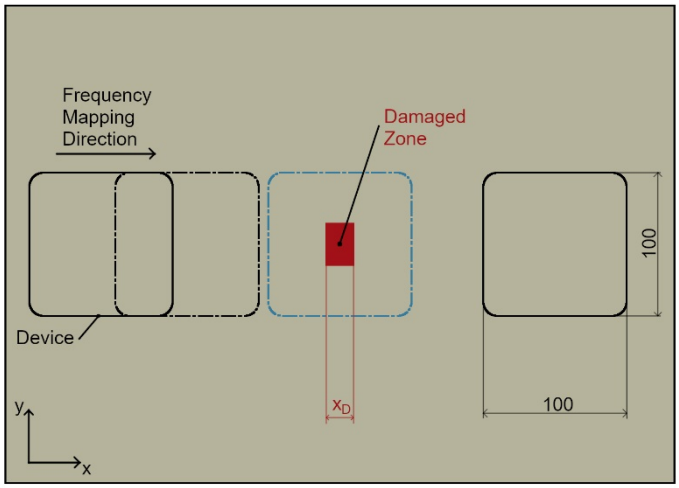

Fig. 4. Frequency mapping procedure.

The presence of a damage within the region inspected through our device results in a reduction of the first resonant frequency. As it will be shown later, such reduction is function of the participation of the damage to the modal displacement. The higher the modal displacement in correspondence of the damaged zone, the higher the reduction of the first resonant frequency. For the first resonance, the higher reduction is obtained when the damage is in the centre of the device. Through the mapping procedure of Fig. 4, the minimum value of the frequency is established.

As the reduction depends on the participation of the damage to the modal displacement, each equivalent elastic property of Eq. (5) can be seen as the average of the corresponding elastic properties of the damaged and undamaged material, weighted on the modal displacement. In the first instance, the modal displacement w of the first resonant frequency can be approximated as:

$$w = \left(\frac{1}{2} + \frac{x}{a}\right)^2 \cdot \left(\frac{1}{2} - \frac{x}{a}\right)^2 \quad (6)$$

where x is the longitudinal coordinate and a is the longitudinal dimension of the device (here 100 mm).

By referring to the longitudinal direction, the average Young modulus weighted on the modal displacement can

be expressed as:

$$E_{11,d}\left(\int_{-\frac{x_D}{2}}^{\frac{x_D}{2}} w\,dx\right)+E_{11,0}\left(\int_{-\frac{a}{2}}^{\frac{a}{2}} w\,dx-\int_{-\frac{x_D}{2}}^{\frac{x_D}{2}} w\,dx\right)=E_{11,eq}\left(\int_{-\frac{a}{2}}^{\frac{a}{2}} w\,dx\right) \tag{7}$$

where $E_{11,d}$ is the longitudinal Young modulus of the damaged zone, whose extension is x_D, as also shown Fig. 4. The extension of the damaged region will be here established through the optic fibre LUNA system [12]. Eq. (7) thus assumes a constant value for the residual elastic properties of the damaged area. From Eq. (7), the longitudinal Young modulus of the damaged zone can be calculated as:

$$E_{11,d}=E_{11,0}-\left(E_{11,0}-E_{11,eq}\right)\left(\frac{\int_{-\frac{a}{2}}^{\frac{a}{2}} w\,dx}{\int_{-\frac{x_D}{2}}^{\frac{x_D}{2}} w\,dx}\right) \tag{8}$$

or, by considering Eq. (5):

$$E_{11,d}=E_{11,0}\left[1-\left(1-\left(\frac{f_d}{f_0}\right)^2\right)\left(\frac{\int_{-\frac{a}{2}}^{\frac{a}{2}} w\,dx}{\int_{-\frac{x_D}{2}}^{\frac{x_D}{2}} w\,dx}\right)\right] \tag{9}$$

Eq. (9) thus permits to assess the residual elastic properties specifically of the damaged zone, once its extension is known. Its validation is performed with tensile tests, as described in the next section.

Tensile tests with optic fibre

In order to validate Eq. (9), tensile tests are performed on specimens cut from the impacted plates around the damaged area. Fig. 5 shows the tensile test setup.

Fig. 5. Tensile test of specimens equipped with optic fibre.

The tensile tests are performed on a servo-hydraulic machine (Instron 8801) equipped with a cell load of 100 kN. The crosshead speed is set equal to 2 mm/min, in accordance with the recommendations of the ASTM standard D3039 [13]. Tests are performed in the elastic regime of the materials. In order to obtain a punctual measure of the strain, specimens are equipped with optic fibre. The optic fibre sensing is managed through the LUNA control system and its strain gauge is set to 0.65 mm. From the measurement of the applied load and of the induced deformation, the longitudinal Young modulus is punctually assessed.

3. Results and discussion

As Eq. (9) requires the first resonant frequency of the undamaged material condition f_0, a mapping procedure is performed before impacting the plate. In particular, the frequency was measured at nine different locations on the plate. The mean value is then assumed for f_0, which is 567.4 Hz and 594.3 Hz for the 6- and 8-layers plates, respectively.

The first resonant frequency is mapped according to the procedure previously described. Measurements are taken by moving the device in the x direction, with steps of about 10 mm. Fig. 6a and 6b report the variation of the first resonance for the 6-layers plate and for the 8-layers plate, respectively. The measured frequencies are plotted according to the position of the central crack of the damaged area with respect to the centre of the device.

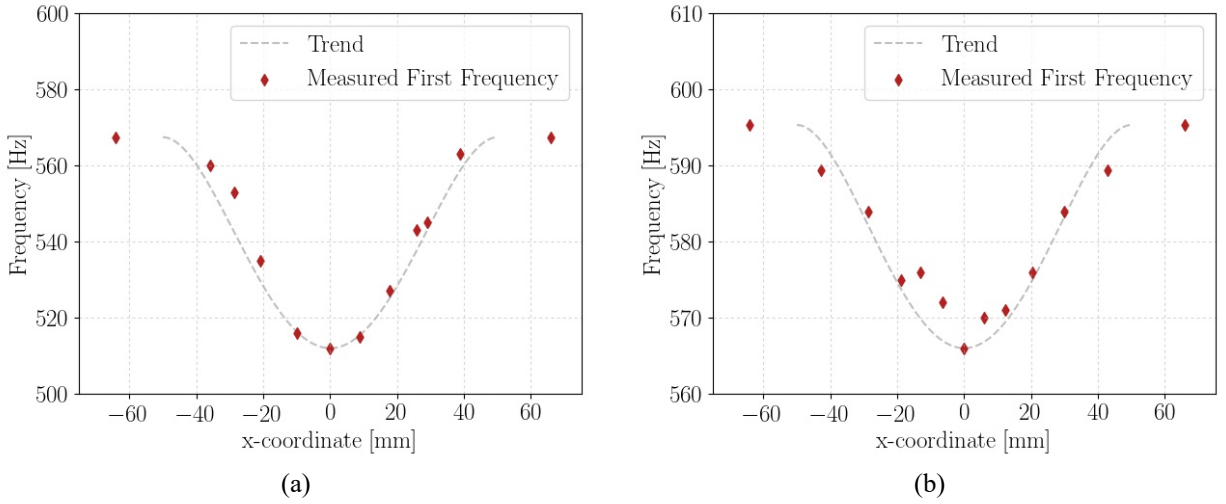

Fig. 6. Frequency trend as a function of the damage position with respect to the device: (a) 6-layers plate; (b) 8-layers plate.

As shown in Fig. 6, the first resonant frequency changes in accordance with the position of the damaged zone with respect to the device boundaries. When the impacted area is external to the system boundaries, no changes occur in the first resonant frequency, thus proving the ability of the system in isolating the vibrational response. By moving the device with respect to the plate, the damage enters the inspected region. At this point the frequency starts decreasing and by further moving the device, the minimum value is reached when the damaged zone is exactly in the centre. The minimum values are 512 Hz for the 6-layers plate and 566 Hz for the 8-laters plate. The reduction of the first resonant frequency is well interpolated through the modal displacement equation (Eq. (6)), as shown with trendline in two diagrams of Fig. 6. This confirms that the participation of the damage to the first mode displacement governs the reduction of the first resonant frequency. Therefore, when the damaged zone is in correspondence of the boundaries, where the displacement is null, no reduction occurs in the first frequency. When the damage is in the centre of the inspected region, its participation to the modal displacement is maximum and so the first resonant frequency falls to the minimum value.

Tensile tests are performed on specimens cut from the impacted plates around the damaged area. Local strains are measured with the optic fibre. Fig. 7a and 7b report the variation of the longitudinal Young modulus E_{11} along the specimen axis for the 6- and 8-layers composites, respectively.

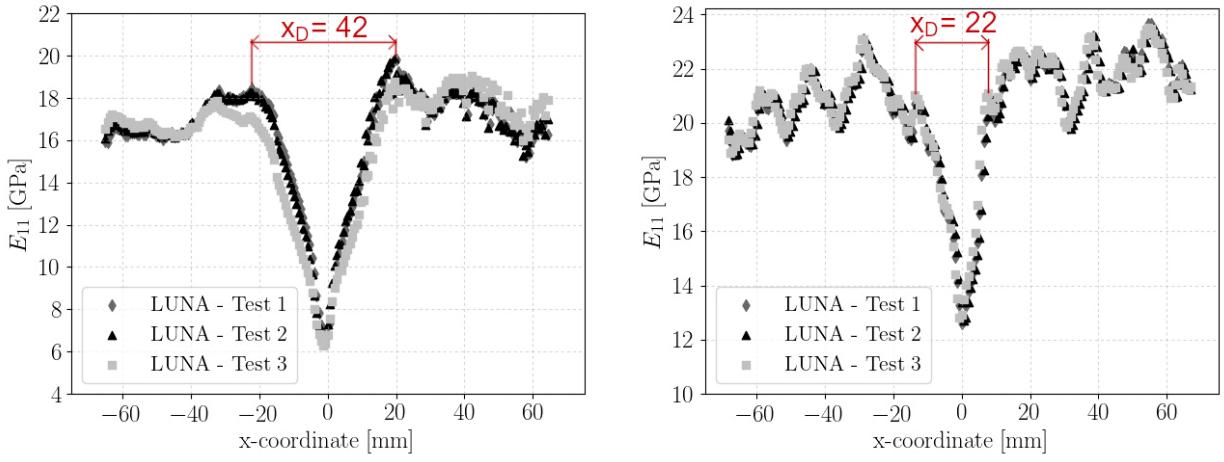

Fig. 7. Young's modulus variation along the specimen axis as measured through the fibre optic: (a) 6-layers composite; (b) 8-layers composite.

The repeatability of results is confirmed through three test repetitions. Both in the 6- and 8-layer plates, in correspondence of the damaged area, the Young modulus progressively decreases to a minimum value. The size of the damaged zone is accordingly identified from the variation of the Young modulus, as shown in Fig. 7. As expected, the size of the damage in the 6-layers is larger than that in the 8-layers, as the impact energy was the same for both the plates. It is also worth noticing that, for both the materials, a severe discrepancy is present between the size of the damaged area estimated by visual inspection, Fig. 3, and that estimated by the optic fibre. For example, in the case of the 8-layers plate, the damage size estimated by the optic fibre is 22 mm, while the extension of the crack in the longitudinal direction is 16.3 mm. This distinction might be due to nonvisible damage mechanisms, such as the plasticization of the matrix. Also, the conceptual distinction between the damage size i.e., that determined by visual inspection, and the portion of material, whose response is affected by the damage, i.e., a "a damage influence size", can help to interpret the discrepancy. Indeed, the size estimated by the optic fibre is also, if not mainly, related to the crack transverse to the applied tensile load, i.e., the 18.8 mm crack and the 10.8 mm crack for the 6-layers and 8-layers plate, respectively. In this viewpoint, the size of the damaged area, estimated by the optic fibre, would correspond to the portion of material which is unloaded because of the presence of the transverse crack. However, further investigations are required in this regard, for example by realizing laminates with defects of known dimension and assessing the material response in presence of such defects.

Table 2 reports a comparison of the results obtained with the optic fibre system and with the local vibrational analysis for the 6- and 8-layers composites.

Table 2. Comparison of the residual elastic properties for the 6- and 8-layers plate.

Material	Method	E_{eq}	E_d
6-layers plate	Fibre Optic	15.0	12.5
	Local Vibrational Analysis	13.7	12.4
8-layers plate	Fibre Optic	20.2	16.6
	Local Vibrational Analysis	19.3	16.4

In order to consistently compare the results, as Eq. (9) assumes a constant value for the residual elastic properties of the damaged area, a mean value for the damaged zone is also calculated from the tensile test results. The discrepancy between the two residual Young moduli values E_d is equal to 1% for both the plates. The very limited difference validates Eq. (9) and proves the accuracy of the technique.

4. Conclusion

In this work, an innovative methodology for the local and nondestructive assessment of the residual elastic properties in damaged composites has been presented. The methodology is based on the Impulse Excitation Technique (IET). An innovative experimental setup which allows to isolate the vibrational response of a region of the material by non-destructively clamping its extremities has been proposed.

The assessment of the residual elastic properties is nondestructive and local, i.e., it specifically concerns the damaged zone. It has been shown that the presence of a damage within the region inspected through the device results in a reduction of the first resonant frequency. Such reduction is function of the participation of the damage to the modal displacement. The higher the modal displacement in correspondence of the damaged zone, the higher the reduction of the first resonant frequency. This allowed to determine the elastic properties specifically of the damaged region, through a properly derived formulation.

The methodology has been validated on two glass fibre woven fabric laminates, damaged by impact. The material properties of the damaged zone determined through the proposed technique have been compared to the results of tensile tests performed on specimens cut from the impacted plates. In particular, the specimens were equipped with optic fibre in order to punctually measure the longitudinal strain and so the elastic parameters. Results show that the residual elastic properties assessed with the proposed technique are in very good agreement with those measured through the optic fibre, thus proving the effectiveness of the methodology.

References

[1] R. Talreja, N. Phan, Assessment of damage tolerance approaches for composite aircraft with focus on barely visible impact damage, Compos. Struct. 219 (2019) 1–7. https://doi.org/10.1016/j.compstruct.2019.03.052.

[2] C. Garnier, M.L. Pastor, F. Eyma, B. Lorrain, The detection of aeronautical defects in situ on composite structures using non destructive testing, Compos. Struct. 93 (2011) 1328–1336. https://doi.org/10.1016/j.compstruct.2010.10.017.

[3] P. Cawley, R.D. Adams, The location of defects in structures from measurements of natural frequencies, J. Strain Anal. 14 (1979) 49–57. https://doi.org/https://doi.org/10.1243/03093247V142049.

[4] A. Zak, M. Krawczuk, W. Ostachowicz, Vibration of a laminated composite plate with closing delamination, J. Intell. Mater. Syst. Struct. 12 (2002) 545–551. https://doi.org/10.1106/9PFK-LXAD-9WLL-JXMG.

[5] H. Hu, J. Wang, Damage detection of a woven fabric composite laminate using a modal strain energy method, Eng. Struct. 31 (2009) 1042–1055. https://doi.org/10.1016/j.engstruct.2008.12.015.

[6] ASTM, Standard Test Method for Dynamic Young's Modulus, Shear Modulus, and Poisson's ratio by Impulse Excitation of Vibration, 2015. https://doi.org/10.1520/E1876-15.responsibility.

[7] D.S. Paolino, H. Geng, A. Scattina, A. Tridello, M.P. Cavatorta, G. Belingardi, Damaged composite laminates: Assessment of residual Young's modulus through the Impulse Excitation Technique, Compos. Part B Eng. 128 (2017) 76–82. https://doi.org/10.1016/j.compositesb.2017.07.008.

[8] C. Boursier Niutta, A. Tridello, G. Belingardi, D.S. Paolino, Nondestructive determination of local material properties of laminated composites with the impulse excitation technique, Compos. Struct. 262 (2021). https://doi.org/10.1016/j.compstruct.2021.113607.

[9] C. Boursier Niutta, Enhancement of a new methodology based on the impulse excitation technique for the nondestructive determination of local material properties in composite laminates, Appl. Sci. 11 (2021) 1–17. https://doi.org/10.3390/app11010101.

[10] R.F.S. Hearmon, The frequency of flexural vibration of rectangular orthotropic plates with clamped or supported edges, J. Appl. Mech. 26 (1959) 537–540.

[11] G.B. Warburton, The Vibration of Rectangular Plates, Proc. Inst. Mech. Eng. 168 (1954) 371–384. https://doi.org/10.1243/pime_proc_1954_168_040_02.

[12] Luna Innovations, https://lunainc.com/, (2021).

[13] ASTM, Standard Test Method for Tensile Properties of Polymer Matrix Composite Materials, 2017. https://doi.org/10.1520/D3039.